Quantum Electronics **46** (6) 548–554 (2016)

STIMULATED LIGHT SCATTERING DOI: 10.1070/QEL15700

Stimulated concentration (diffusion) light scattering on nanoparticles in a liquid suspension

I.S. Burkhanov, S.V. Krivokhizha, L.L. Chaikov

Abstract. **A nonlinear growth of the light scattering intensity has been observed and the frequency shift of the spectral line of scattered light has been measured in light backscattered in suspensions of diamond and latex nanoparticles in water. The shift corresponds to the HWHM of the line of spontaneous scattering on particles. We may conclude that there exists stimulated concentration (diffusion) light scattering on variations of the particle concentration, which is also called the stimulated Mie scattering. In a fibre probe scheme, the growth of the shift of the scattered spectral line is observed with an increase in the exciting beam power. The variation of the frequency shift with an increase in the exciting power is explained by convection in liquid.**

Keywords: *stimulated light scattering, diffuse scattering, concentration scattering, stimulated Mie scattering, nanoparticles, liquid, correlation spectroscopy.*

1. Introduction

Each type of classical (spontaneous) light scattering (CLS) has an analogue in the form of stimulated scattering (SS). Thus, for the CLS caused by fluctuations/variations of phased molecule excitation, it is stimulated Raman scattering (SRS) [1]; for CLS caused by pressure fluctuations/variations [2, 3], it is stimulated Brillouin scattering (SBS); for CLS caused by anisotropy fluctuations/variations, it is stimulated Rayleigh-wing scattering (SRWS) [4–6]; for CLS caused by entropy fluctuations/variations, it is stimulated thermal scattering (STS) [3, 7–9]. Recently, stimulated globular scattering (SGS) has been discovered, i.e., a low-frequency Raman scattering caused by eigenvibrations of particles [10, 11]. The spectral shift of the SGS line is in the range of 12–20 GHz. There is also stimulated concentration scattering (SCS) caused by fluctuations/variations of the concentration of particles or mixture components.

Spectral lines of the spontaneous Brillouin scattering and of Raman scattering are shifted relative to the exciting line, lines of SRS and SBS being shifted by approximately the same value. The lines of spontaneous depolarised Rayleigh scattering (caused by anisotropy fluctuations) and of scattering by entropy fluctuations are not shifted relative to the line of exciting light; they are only broadened. However, SRWS and STS lines are shifted relative to the exciting radiation line by approximately half the width of the line of the corresponding CLS. This shift is related to the fact that the STS and SRWS gains are proportional both to the coefficient of spontaneous scattering and to the density of states that linearly depends on the frequency shift. Thus, the frequency shift of scattered light equal to half the line width of spontaneous scattering is the most important indication to the emergence of SS. One more important indication to SS is a nonlinear growth of the scattered light intensity under an increasing intensity of the exciting light.

There have been numerous attempts to study SCS, which is an analogue of spontaneous concentration scattering (SpCS) caused by concentration fluctuations in materials constituting a solution. Thus, in binary gaseous mixtures [12] in the scheme employing a high-power laser and super-regenerative amplification of scattered light by using a Fabry–Perot interferometer, a line with the frequency shift of 0.033–0.042 cm^{-1} has been found in the spectrum of scattered light, which the authors attributed to SpCS. Bloembergen et al. [13] have measured the frequency shift for SCS in a He–Xe mixture and a He–SF_6 mixture, which was 0.005–0.022 cm^{-1} and 0.005–0.018 cm^{-1}, respectively. The corresponding theory has been developed basing on these experiments [14].

Attempts to measure SCS in water solutions of latidine were made in [15] but at a spectral resolution of 0.003 cm^{-1}, measurements of the frequency shift of scattered light failed. However, using the time evolution of the scattering intensity the authors concluded that there was stimulated scattering at an unshifted frequency, which was interpreted as SCS.

There were attempts to observe SCS on gold nanotubes with a diameter of 13 nm and a length of 90 nm in water, on CdSe/CdS/ZnS nanocrystals in chloroform and on Au, Au/Ag, Ag and Pt nanoparticles with a size of 10 nm in toluene [16–18]. However, in these suspensions the authors also failed to measure the shift of the SS spectral line at the resolution of up to 0.005 cm^{-1}, although they observed the nonlinear growth of backward scattering. By an increase in the intensity and the appearance of a specific peak on the temporal dependence of the SS intensity, the authors of [16–20], as in [15], made a conclusion about the observation of SS on particles.

SCS in liquids can also be termed stimulated diffusion light scattering (SDLS) because its frequency shift and the relaxation time of particle concentration fluctuations are determined by their diffusion coefficient. SCS on variations of particle concentrations in liquids is often called stimulated Mie scattering [16–20].

I.S. Burkhanov, S.V. Krivokhizha P.N. Lebedev Physics Institute, Russian Academy of Sciences, Leninsky prosp. 53, 119991 Moscow, Russia; e-mail: ilyaburkhanov@gmail.com, skrivokh@sci.lebedev.ru; **L.L. Chaikov** P.N. Lebedev Physics Institute, Russian Academy of Sciences, Leninsky prosp. 53, 119991 Moscow, Russia; National Nuclear Research University 'MEPhI', Kashirskoe shosse 31, 115409 Moscow, Russia; e-mail: chaik@sci.lebedev.ru

Received 24 October 2014; revision received 4 February 2016
Kvantovaya Elektronika **46** (6) 548–554 (2016)
Translated by N.A. Raspopov

Thus, the frequency shift for SCS was only measured in gas mixtures. Measurements of the frequency shift and its observation failed both in liquid solutions and in suspensions of particles in liquids, because in liquid solutions the HWHM of the line of backward spontaneous scattering (and the value of the spectral shift of the SS line) is 0.3–3 MHz, which is substantially less than in gases. For particles in liquids this value is even less and equals 30–12000 Hz. The authors of [15–20] used a conventional method for spectral measurements of SS by a Fabry–Perot interferometer, which had an *a fortiori* insufficient resolution for detecting the frequency shifts mentioned above.

The method of correlation spectroscopy is suitable for measuring such shifts. It is capable of measuring frequency shifts down to several hertz. In this case, a cw exciting laser should be used instead of a high-power pulse laser conventionally employed in SS investigations.

We have earlier tried to detect a frequency shift and the nonlinear growth of the SDLS intensity by using a cw laser and a correlator in studying suspensions of silica nanoparticles in oil and diamond aggregates in water [21].

The present work is aimed at detecting, under an increasing intensity of the exciting light, the nonlinear growth of the scattering intensity and observing the line in its spectrum shifted in frequency by half the width of the CLS line in suspensions of diamond aggregates and certified latex nanoparticles in water. In this way we can demonstrate the origin of SCS (SDLS, stimulated Mie scattering) [22] and study features of its appearance in various optical schemes.

2. Method of dynamic light scattering in investigations of SCS (SDLS)

In the case of SCS, the exciting and scattered waves interfere, and an interference intensity grating is produced, in antinodes (or minima) of which the particles of suspension are involved (see, for example, [23, 24]). As a result, a concentration grating of particles and, consequently, of the refractive index is formed [23]:

$$N(z, t) = N_0 + \delta N(t)\exp(-\mathrm{i}\Omega t + \mathrm{i}|\boldsymbol{k}_\mathrm{L} - \boldsymbol{k}_\mathrm{S}|z). \qquad (1)$$

Here, $N(z, t)$ and N_0 are the local and average concentrations of particles; $\delta N(t)$ is the concentration grating amplitude; Ω is the frequency shift of the SS spectral line; z is the coordinate along the propagation direction of the exciting wave; and $\boldsymbol{k}_\mathrm{L}$ and $\boldsymbol{k}_\mathrm{S}$ are the wave vectors of the exciting and scattered light, respectively. The concentration grating (1) moves at a velocity of $V_\mathrm{gr} = \Omega/q$, $\boldsymbol{q} = \boldsymbol{k}_\mathrm{S} - \boldsymbol{k}_\mathrm{L}$ is the wave vector of scattering.

The HWHM of the non-shifted line of light spontaneously scattered by particles in a liquid is $\Gamma_1 = Dq^2$, where D is the diffusion coefficient for particles in a liquid; thus, the process of SCS (SDLS) should produce a line in the spectrum of scattered light that is shifted by the same value $\Omega = Dq^2$ (similarly to the case of STS). For the particles of radius 480 nm in water this shift should be $\sim$500 s^{-1} or 80 Hz. Such a shift can be detected by the method of correlation spectroscopy, whereas with Fabry–Perot interferometers it is impossible.

If the scattered light that passes to a quadratic photodetectorcomprises two spectral components shifted by $\Delta\omega$ to each other, then a cosine component should arise in the correlation function of the scattered light intensity due to the frequency beating. Similarly to [25], one can obtain the expression for the correlation function of the scattered intensity in the case of beatings between the reference wave (I_h) and the line of stimulated scattering (I_2) in the presence of the spontaneous scattering line (I_1) [21]:

$$G^{(I)} = (\tau)\langle I(t)I(t+\tau)\rangle = I_1^2\exp(-2\Gamma_1\tau) + I_2^2\exp(-2\Gamma_2\tau) + 2I_1I_\mathrm{h}\exp(-\Gamma_1\tau) + 2I_2I_\mathrm{h}\exp(-\Gamma_2\tau)\cos(\Omega\tau) + \langle I_1 + I_2 + I_\mathrm{h}\rangle^2, \qquad (2)$$

where $G^{(I)}(\tau)$ is the correlation function of the scattered light intensity; Γ_2 is the HWHM of the SS line; in the case of plane waves and steady-state regime, we have $\Omega = \Gamma_1 = Dq^2$. For a stimulated process, with the growth of the exciting light intensity the intensity of the shifted line should increase exponentially; at small intensities it should increase quadratically.

3. Samples and experimental setup

In SCS (SDLS) investigations we used two types of samples: suspensions of diamond nanoparticle aggregates in water and water suspensions of monodisperse latexes.

Samples of the diamond suspension were prepared from diamond paste by multiple dilution in dust-free twice-distilled water. According to the producer's characteristics, the diamond paste comprised diamond nanoparticles of size 2–4 nm. After dilution, the solution had aggregates of diamond nanoparticle of size 100–1200 nm (Fig. 1). Results given below refer to a suspension with aggregates having an average effective radius of 488±8 nm and a volume concentration of $C_V = 4\times10^{-5}$% [21]. However, actually the suspension comprises particles with radii of 106 and 1200 nm (Fig. 1). This distribution of the scattering intensity over particle radii is obtained by the method of dynamic light scattering at low intensities of the exciting light (λ = 532 nm, P = 0.89 mW).

From Fig. 1 one can see that the maximum light scattering corresponds to particles with the radius of 1193 nm. It is possible to determine that such aggregates, as was earlier shown in [26], include not only diamond but also water; the volume content of the latter being approximately 60%–70%.

Suspensions of latex samples were prepared from monodisperse suspensions of spherical latex particles in water produced at the Institute of Synthetic Rubber with a narrow size distribution and an initial weight concentration of 6%. Particle radii were 80 and 480 nm. Using an analytical balance these latexes were diluted in twice-distilled dust-free water to volume concentrations of $C_V = 5\times10^{-3}$% and 0.7×10^{-3}% and then poured into special dust-free cells. For the particles with a radius of 480 nm at $C_V = 7\times10^{-4}$% the concentration of particles was $N_\mathrm{p} = 1.5\times10^7$ cm^{-3} and the average distance between them was 40 μm.

Scattering in suspensions of diamond nanoparticles was investigated in the classical optical scheme of backward scattering [21, 27], where instead of a conventionally employed powerful pulsed laser, a solid-state cw laser was used with a radiation wavelength of 532 nm, radiation power of up to 50 mW, radiation divergence of 0.5 mrad, and beam diameter of 2 mm. The power of pump radiation was controlled by two polarises: a Frank–Ritter prism and film polariser. The film polariser provided variation of the exciting radiation power without shifting the beam. Then the light passed through a semitransparent (with the transmission of 50%) mirror was focused to a cell with the suspension in question by a lens with a focal length of 30 mm. Light scattered backward returned to

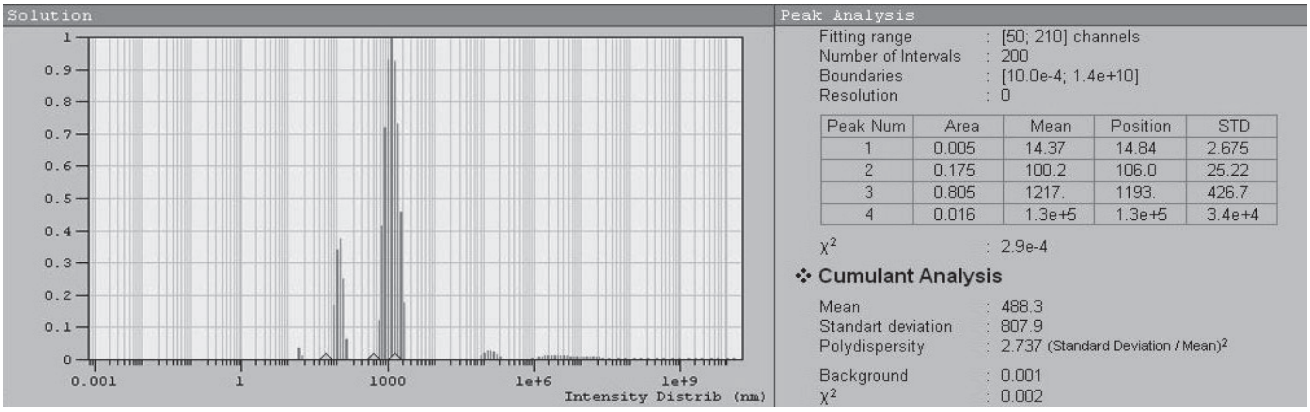

Figure 1. Results of employing the DynaLS programme for processing the correlation function of the backscattered light in a suspension of diamond nanoparticles in the case of absent SS (the laser power is 0.89 mW). Histogram of the scattering intensity distribution over particle radii (left) and numerical results (right).

the semitransparent mirror, reflected from it and after passing an aperture diaphragm was focused by an objective to a cathode diaphragm placed in front of a photoelectron multiplier. These diaphragms provided the spatial coherence of scattered light. A signal from a photoelectron multiplier passed to a Photocor FCm correlator (Antek-97, now Photocor).

Adjustment of the installation is sufficiently complicated; therefore, we used an optical scheme that is simpler in practice, namely the scheme with a fibre probe (Fig. 2).

The same cw solid-state laser was used as a light source. The laser radiation at a wavelength of $\lambda = 532$ nm after polariser P3, which controlled the power of exciting radiation, was brought by lens L3 with the focal length of 15 mm to an illuminating fibre of the fibre probe. The output end of the illuminating fibre was embedded into a single thin cylindrical block, formed as a probe, together with an input end of the collecting fibre. These fibres were parallel and a distance between their axes was 0.3 mm. The probe was plunged into a cell with a suspension to be studied. Radiation scattered in a volume near the probe end was transported from the cell through the collecting fibre. At the output from the collecting fibre this radiation passed through a polariser P2 and a system providing spatial coherence (SCohS) to the cathode of the same PEM that was used in the classical optical scheme for backscattering measurements. The SCohS comprised an aperture and cathode diaphragms and a lens L2. The scheme with fibre probes required minimal adjustment. One should merely ensure light passing to the illuminating fibre, bring the image of the end of the collecting fibre with the diaphragm, and see that the light from the fibre probe did not fit walls of the cell. Light reflected from a vessel bottom was a reference wave.

In order to clarify the role of convection and to measure its velocity, a He–Ne laser, vertical beam splitter BS, and lenses L1 with a focal length of 10 or 30 cm forming the conventional Doppler double-beam scheme (see, for example, [28]) were introduced into the optical scheme. Light scattered at a small angle relative to the axis of the He–Ne laser in the horizontal plane was focused by the objective through a red filter to the end of the DS fibre and passed to the SCohS. By

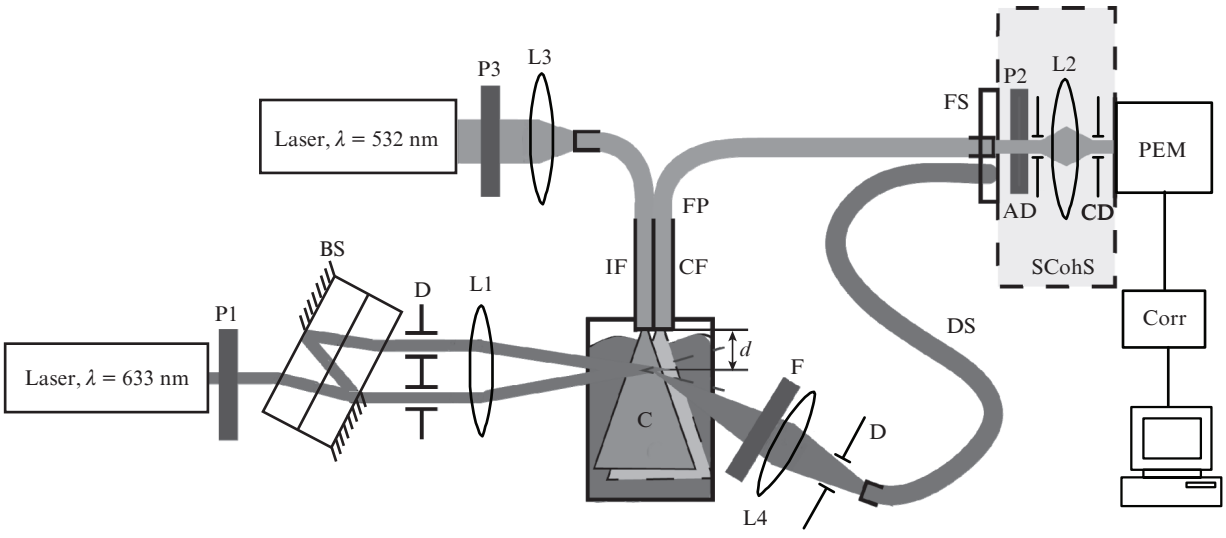

Figure 2. Optical diagram of the experimental setup with a fibre probe: (P1–P3) polarisers; (L1–L4) lenses; (FP) fibre probe; (IF) illuminating probe; (C) cuvette; (CF) collecting fibre; (FS) fibre switch; (SCohS) system providing spatial coherence; (AD) aperture diaphragm; (CD) cathode diaphragm; (Corr) correlator; (BS) 50%/50% beam splitter; (D) diaphragms; (F) red filter; (DS) optical fibre transmitting a Doppler signal; $d \approx 2.5$ mm.

simply switching the collecting or DS fibres at the input to the SCohS it is easy to transfer from detection of scattered light to measurements of a vertical velocity of the flow.

In a steady state regime of scattering, the correlation functions of the scattered green light, passed through the CF, were measured with the fibre directed down or up. Then the correlation functions of the scattered light of two beams of the He–Ne laser that have passed through the DS (Fig. 2) were measured. The period T of the cosine of correlation functions for scattered light from two beams of the He–Ne laser yields the value of the convection flow velocity:

$$V_c = \Lambda/T = \lambda/[2T\sin(\alpha/2)], \quad (3)$$

where Λ is the wavelength of the interference fringe in the intersection domain of He–Ne laser beams; λ is the wavelength of laser radiation; and α is the convergence angle for the beams in air.

The velocity of the convection flow was measured at a distance of ~2.5 mm from the fibre probe end. This value estimated from the dependences of the exciting radiation intensity on the distance and from the area of intersection of the light cones with the field of view of the fibre is considered as the most efficient for detecting SS.

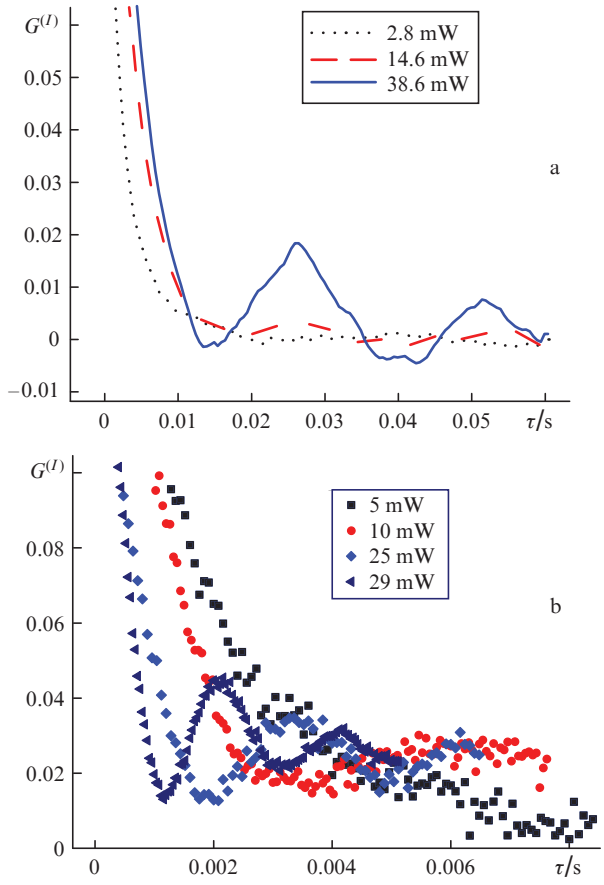

Figure 3. Correlation functions of light backscattered (a) by a suspension of aggregates of diamond nanoparticles with a radius of 1200 nm in water at the exciting radiation power of P_{las} = 2.8, 14.6 and 36.8 mW (the classical backscattering scheme, steady-state regime) and (b) by a suspension of latex particles with a radius of 480 nm at P_{las} = 5, 10, 25 and 29 mW [the fibre scheme of backscattering (Fig. 2), steady-state regime].

4. Experimental results

The correlation functions of light scattered by suspensions of aggregates of diamond nanoparticles in the classical optical scheme and by latex nanoparticles in the fibre probe backscattering scheme were measured. It was found that at increasing the power of the exciting light, the form of the correlation function of intensity $G^{(I)}(\tau)$ changes. It acquires a cosine component (Fig. 3), which testifies that the line arises in a scattering spectrum shifted by the frequency Ω relative to the frequency of the exciting light [see (2)] [21, 27].

It turns out that an amplitude of the cosine component (at I_h = const) rises with an increase of P_{las} (Fig. 3) [27], and the SS intensity I_2 depends exponentially on I_{las} (Fig. 4). The total intensity of the backscattered light is well approximated by the expression $I_{sca} = A\exp(gLI_{las}) + BI_{las}$, where the last term includes the intensity of the reference wave; g is the gain; and L is the length of interaction.

The nonlinearity of scattering is better demonstrated by the ratio of the intensity of scattered light I_{sca} to the power of the exciting light P_{las} (Fig. 5). From this figure one can see that the scattered light intensity grows quadratically or even faster.

The correlation functions of the scattered light intensity obtained in SS for the radiation with λ = 532 nm were approximated by the expression

$$\ln G^{(I)}(\tau) = \ln[C\exp(-2G_1\tau) +$$

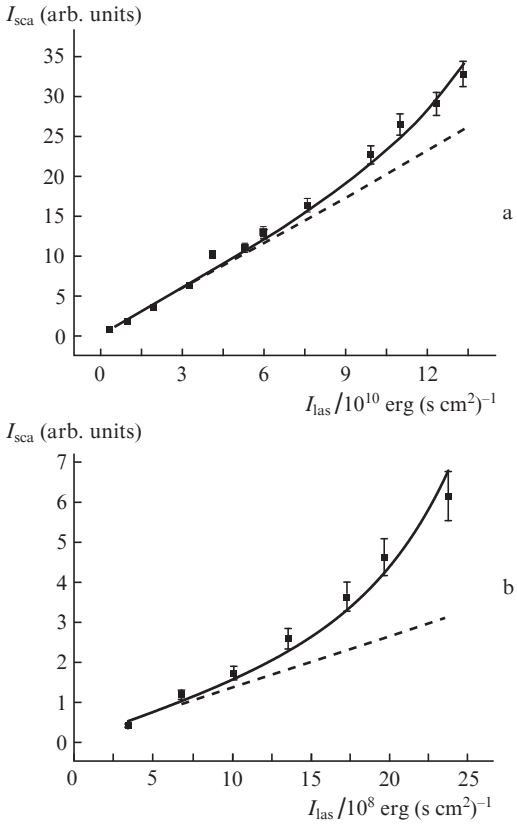

Figure 4. Total intensity of scattered light I_{sca} vs. the intensity of exciting light I_{las} (a) in a suspension of diamond nanoparticles in water (the classical backscattering scheme, [21]), $C_V = 4\times10^{-5}$%, and (b) in an emulsion of latex particles of radius 480 nm in water (the fibre probe scheme, Fig. 2 [25]), $C_V = 5\times10^{-3}$%. The linear part of I_{sca} is plotted with dashed lines.

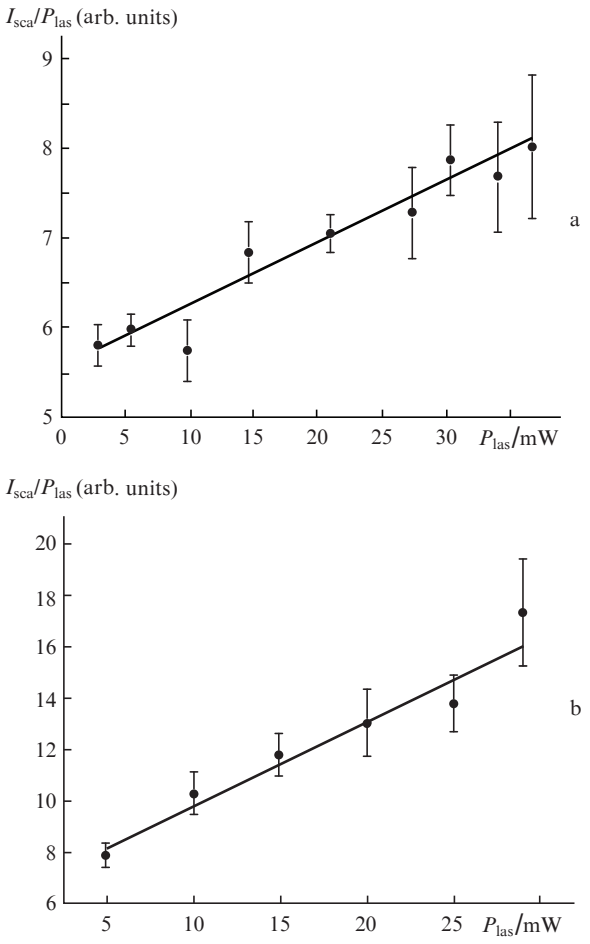

Figure 5. Ratio I_{sca}/P_{las} vs. P_{las} (a) for a suspension of diamond nanoparticles in water (the classical backscattering scheme, [21]) and (b) for an emulsion of latex particles of radius 480 nm in water (the fibre probe scheme, Fig. 2).

$$+ D\exp(-2G_2\tau)\cos(\Omega\tau) + F]. \qquad (4)$$

The approximation yields the values of Ω in the range of 230–248 s^{-1} for the suspensions of diamond aggregates. These values exhibit no regularity law with increasing P_{las} and in the average (taking into account measurement errors) are 240 ± 20 s^{-1}, which slightly differs from the theoretical value that equals to HWHM of the line of spontaneous scattering $Dq^2 = 209$ s^{-1}; however, these values are very close.

The widths of stimulated scattering Γ_2 are actually independent of the power P_{las} and in the emulsion of diamond nanoparticle aggregates are within 50 ± 6 s^{-1} and in the emulsion of latex particles with the radius of 480 nm are 325.0 ± 13.2 s^{-1}.

However, the values of Ω for latex particles in the fibre probe scheme of measurements grow from 750 to almost 2800 cm^{-1} with an increase in P_{las} from 10 to 29 mW. Although in the suspension of particles with the radius of 480 nm at 25 °C the line HWHM of spontaneous backscattering is $\Gamma_1 = 504$ s^{-1}, the shift Ω of the SS line should be the same and in the frameworks of the stationary model should not depend on the intensity of exciting radiation. It was found that the difference between the experimental results and theoretical predictions is related to the arising convection.

5. Influence of convection

Latex particles, as compared to diamond nanoparticles, possess a greater absorption coefficient at $\lambda = 532$ nm. It is sufficient for producing a convection flow in a cell with the suspension. The velocity of such a flow V_c increases with increasing P_{las} and its dependence on the vertical coordinate has a maximum at a distance of ~2.4 mm from the end of fibres. In the suspension of latex particles with the radius of 480 nm and the concentration of $C_V = 7 \times 10^{-4}$% under the variation of laser power from ~5 to 33 mW the velocity V_c at the distance of 2.4 mm from fibre ends varied from ~0.005 to 0.05 cm s^{-1} (Fig. 6a). In this case, the Doppler shift due to the particle movement in the flow along the beam is added to the frequency shift of the SS line; thus, the correlation function for the intensity of backscattered light changes as compared to (2):

$$G^{(I)}(\tau) = I_1^2\exp(-2\Gamma_1\tau) + I_2^2\exp(-2\Gamma_2\tau) + 2I_1I_h \times \exp(-2\Gamma_1\tau)\cos(\Omega_c\tau) + 2I_2I_h\exp(-2\Gamma_2\tau) \times \cos(\Omega_m\tau) + \langle I_1 + I_2 + I_h\rangle^2. \qquad (5)$$

Here, $\Omega_m = \Omega_{st} + \Omega_c$ is the total measured shift of the SS line; $\Omega_c = 4\pi n V_c/\lambda$ is the shift due to the convective flow; Ω_{st} is the shift due to SS; n is the refractive index of water.

However, at a minimal laser power where SS is yet below the detection limit, the period T_{min} of the function $\cos(\Omega_c\tau)$ related with a convective flow is 55.3×10^{-3} s and $\tau_D = (\Gamma_1)^{-1}$ is 2.1×10^{-3} s. In this case, the first maximum of the correlation function relative to the amplitude of the latter, $\exp(-\Gamma_1 \times T_{min})$, equals 0.08 and actually cannot be observed. At increasing the laser power, the period T reduces; however, I_2 sharply (quadratically or faster) rises. Hence, the influence of $\cos(\Omega_c\tau)$ on the value of correlation functions reduces and we still approximate them by formula (4).

Results of measurements of the velocity of convective flow V_c and the total shift Ω_m of the SS line versus the laser power are shown in Fig. 6.

The grating of the refractive index (and of particle concentration), on which SS occurs, moves relative to a liquid at a velocity of $V_{gr} = c\Omega_{st}/2\omega_0 = \Omega_{st}\lambda/4\pi n$ (ω_0 is the circular frequency of the light wave). It was found that the velocity of convection V_c is higher than the velocity of the grating V_{gr}. The Doppler shift Ω_c related with the convective flow is equal to $4\pi n V_c/\lambda$. Under the assumption of simple summation of the velocities of the grating and convective flow, if the light probe is directed down in the case of Stokes SS, we have $\Omega_m^{down} = \Omega_c - \Omega_{st}$ ($V_m = V_c - V_{gr}$). If the light probe is directed up, we have $\Omega_m^{up} = \Omega_c + \Omega_{st}$ because the directions of the shifts coincide (Fig. 7).

In Fig. 8 we present the result of subtracting the Doppler shift, related to the velocity of the convective flow Ω_c, from the measured frequency shift of the SS line Ω_m shown in Fig. 6 versus the power of exciting radiation.

One can see that in the range of the developed SCS ($P_{las} >$ 20 mW) the experimental values of Ω_{st} obtained in this way verge towards the theoretical value $\Omega_{st} = Dq^2 = 504$ s^{-1} for the down direction of the light probe (and –504 s^{-1} for the up direction), although being slightly above it as in the case of diamond. The reduction of Ω_{st} under a decrease in P_{las} is, seemingly, explained by an influence of the third term with $\cos(\Omega_c\tau)$ in (5), which has not been taken into account in approximating the correlation function.

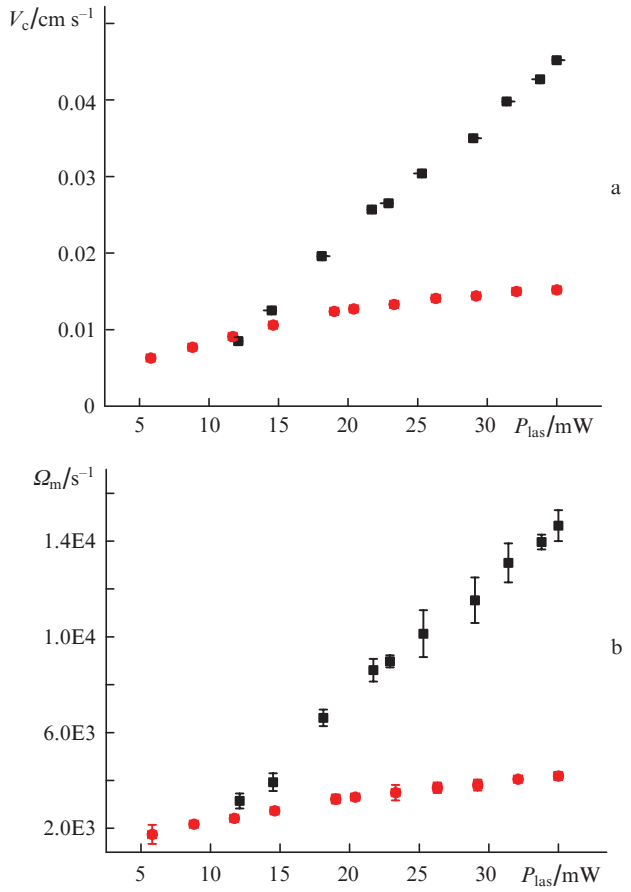

Figure 6. (a) Convection velocities V_c and (b) measured total SS frequency shifts Ω_m vs. the laser radiation power for a suspension of latex particles of radius 480 nm in water at the concentration $C_V = 7 \times 10^{-4}$% in the case where the fibre probe is directed down (●) and up (■).

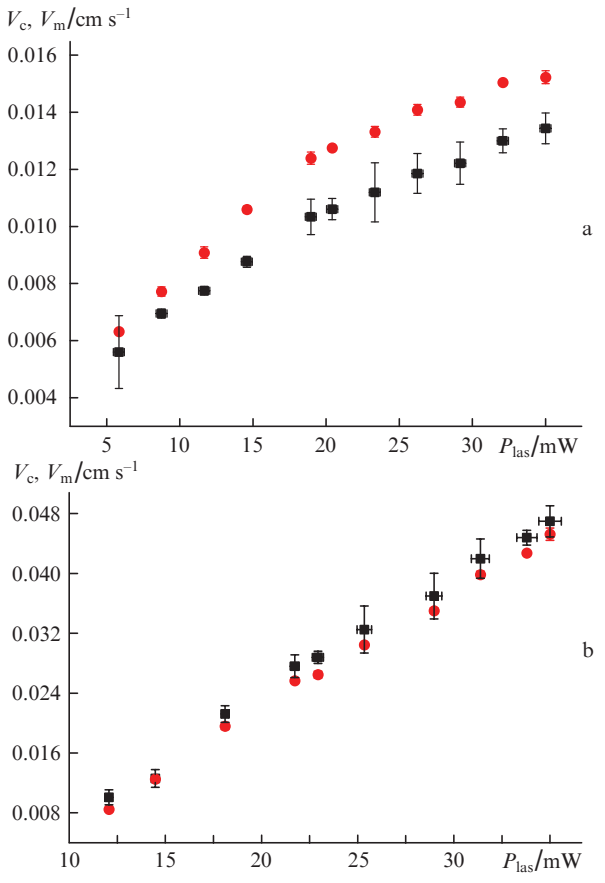

Figure 7. Dependence of the total lattice velocity $V_m = \Omega_m \lambda/4\pi n$ (■) and the velocity of convection V_c (●) for a suspension of latex particles of radius 480 nm in water at the concentration of $C_V = 7 \times 10^{-4}$% in the case where the fibre probe is directed (a) down and (b) up.

The frequency shift of the SS line (the frequency of the maximal gain) may also slightly vary due to distortions of the frequency dependence of the SS gain, similarly to the case of the four-wave interaction in a moving medium [29]. However, this fine effect is not considered in the present work.

The approximation of the dependence of scattered light intensity on the intensity of exciting radiation by the formula $I_{sca} = A\exp(gLI_{las}) + BI_{las}$ given in Fig. 4 yields for the SCS gain in a suspension of latex particles with the radius of 480 nm the values $g_{lat} = (6.5 \pm 2.4) \times 10^{-9}$ s cm erg^{-1} at $L = 0.3$ cm. In the suspension of diamond nanoparticle aggregates in water at $L = 0.042$ cm the corresponding value is $g_d = (1.22 \pm 0.23) \times 10^{-10}$ s cm erg^{-1}. Authors in [23] obtained for g the expression that can be presented in the form more convenient for estimates:

$$g = \frac{64\pi^3}{3c}\frac{1}{\lambda n\eta}\frac{1}{qR}(\sin qR - qR\cos qR)\alpha_0^2 C_V \frac{\Omega_{st}}{(Dq)^2 + \Omega_{st}^2}, \quad (6)$$

where c is the velocity of light; η is the viscosity of water; R is the radius of particles; $\alpha_0 = (3/4\pi)n(m^2 - 1)/(m^2 + 2)$ is the polarisability of medium; and m is the relative refraction index of the particle material.

This expression in the case of our suspension with latex particles at $C_V = 5 \times 10^{-5}$ yields the value $g_{tlat} = 3.5 \times 10^{-9}$ s cm erg^{-1}, and for the diamond suspension under the assumption that diamond aggregates comprise 70% of water this value is $g_{td} = 5.0 \times 10^{-10}$ s cm erg^{-1}. At an available level of the accuracy of estimating L, the agreement between the experimental g_{lat} and theoretical g_{tlat} values for latex can be considered quite satisfactory. As for the diamond suspension, it seems that due to a low convection in the direction normal to the beam axis the concentration lattice simply had not enough time to achieve a stationary level, this is why we have $g_d < g_{td}$.

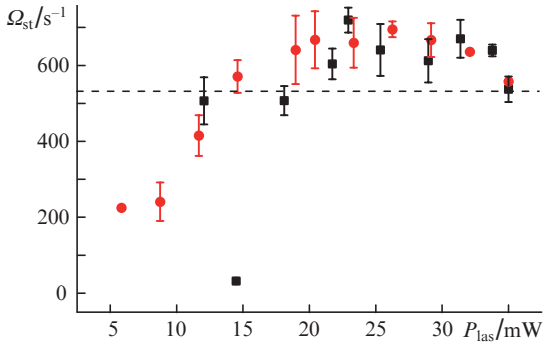

Figure 8. Dependence of $\Omega_{st} = |\Omega_m - \Omega_c|$ on the power of exciting radiation based on results from Fig. 6. The horizontal line corresponds to $\Omega_{st} = \Gamma_1 = 504$ s^{-1}, the fibre probe is directed down (●) and up (■).

Similarly to the phenomena occurring in STS and SRWS, all these facts give grounds to believe that we deal with stimulated light scattering on variations of particle concentration in liquid, that is, stimulated concentration (diffusion) light scattering or stimulated Mie scattering.

Seemingly, the origin of a convective flow prevented us from observing SCS (SDLS) in latex suspensions in the classical backscattering scheme because at the exciting radiation power of 30 mW the time of the concentration grating formation is several seconds, whereas the time of crossing the diameter of the fibre by a convective flow is 0.1 s. Thus, a suspension passes the illuminated domain faster than the concentration lattice arises on which SCS occurs.

6. Conclusions

A nonlinear growth of the scattering intensity has been observed in light backscattered in suspensions of diamond aggregates and latex nanoparticles in water at the intensity of exciting laser radiation of above 100 W cm^{-2} and the radii of suspension particles of 1200 and 480 nm. In the conventional backscattering scheme, the frequency shift of the spectral line of scattered light was observed, which corresponds to the HWHM of the line of spontaneous scattering. In the fibre probe scheme, the shift of the spectral line of scattering was observed, which corresponds to the sum (or the difference in the case of the fibre directed down) of the velocities of the concentration grating $V_{gr} = Dq^2\lambda/4\pi n$ and the convective flow V_c.

Thus, we may assert that in the suspensions under study in the conditions of our experiments, the stimulated concentration (diffusion) light scattering caused by variations of the particle concentration is observed, or stimulated Mie scattering. By using a cw laser and a correlator, we have measured the corresponding frequency shift, which did not exceed the value predicted theoretically by more than 15%.

References

1. Sushchinskii M.M. *Vynuzhdennoe kombinatsionnoe rasseyanie sveta* (Stimulated Raman scattering) (Moscow: Nauka, 1985).
2. Chiao R.Y., Townes C.N., Stoioheff B.P. *Phys. Rev. Lett.*, **12** (21), 592 (1964).
3. Starunov V.S., Fabelinskii E.L. *Usp. Fiz. Nauk*, **98**, 441 (1969) [*Sov. Phys. Usp.*, **13**, 428 (1970)].
4. Mash D.I., Morozov V.V., Starunov V.S., Fabelinskii E.L. *Pis'ma Zh. Exp. Teor. Fiz.*, **2**, 41 (1965) [*JETP Lett.*, **2** (1), 25 (1965)].
5. Sogomonian S., Barille R., Rivoire G. *Opt. Commun.*, **157**, 182 (1998).
6. Zaitsev G.I., Kyzylasov Yu.I., Starunov V.S., Fabelinskii I.L. *Pis'ma Zh. Exp. Teor. Fiz.*, **6** (2), 505 (1967) [*JETP Lett.*, **6** (2), 35 (1967)].
7. Jirauschek C., Jeffrey E.M., Faris G.W. *Phys. Rev. Lett.*, **87** (23), 233902 (2001).
8. Zaitsev G.I., Kyzylasov Yu.I., Starunov V.S., Fabelinskii I.L. *Pis'ma Zh. Exp. Teor. Fiz.*, **6** (8), 802 (1967) [*JETP Lett.*, **6** (8), 255 (1967)].
9. Starunov V.S. *Zh. Exp. Teor. Fiz.*, **57**, 1012 (1969).
10. Gorelik V.S., Kudryavtseva V.S., Chernega N.V. *Kr. Soobshch. Fiz. FIAN*, (11), 43 (2006) [*Bull. Lebedev Phys. Inst.*, **33** (4), 33 (2006)].
11. Tareeva M.V., Gorelik V.S., Kudryavtseva V.S., Chernega N.V. *Kr. Soobshch. Fiz. FIAN*, (11), 3 (2010) [*Bull. Lebedev Phys. Inst.*, **37** (11), 331 (2010)].
12. Aref'ev I.M., Morozov V.V. *Pis'ma Zh. Exp. Teor. Fiz.*, **9**, 448 (1969).
13. Lowdermilk W.H., Bloembergen N. *Phys. Rev. A*, **5**, 1423 (1972).
14. Bloembergen N., Lowdermilk W.H., Matsuoka M., Wang C.S. *Phys. Rev. A*, **3** (1), 404 (1971).
15. Davydov M.A., Shipilov K.F. *Pis'ma Zh. Exp. Teor. Fiz.*, **52** (3), 789 (1990).
16. Guang S.He, Ken-Tye Yong, Jing Zhu, Prasad P.N. *Phys. Rev. A*, **85**, 043839 (2012).
17. Guang S.He, Wing-Cheung Law, Liwei Liu, Xihe Zhang, Prasad P.N. *Appl. Phys. Lett.*, **101**, 011110 (2012).
18. Guang S.He, Wing-Cheung Law, Baev A., Sha Liu, Swihart M.T., Prasad P.N. *J. Chem. Phys.*, **138**, 024202 (2013).
19. Shi J., Wu H., Liu J., Li S., He X. *Sci. Rep.* **5**, 11964 (2015).
20. Shi J., Wu H., Yan F., Yan F., Yang J., He X. *J. Nanopart Res.*, (2016); doi 10.1007/s11051-016-3333-1.
21. Burkhanov I.S., Chaikov L.L. *Kr. Soobshch. Fiz. FIAN*, **39** (3), 22 (2012) [*Bull. Lebedev Phys. Inst.*, **39** (3), 77 (2012)].
22. Zel'dovich B.Ya., Sobelman I.I. *Usp. Fiz. Nauk*, **101** (1), 3 (1970) [*Sov. Phys. Usp.*, **13**, 307 (1970)].
23. Afanas'ev A.A., Rubinov A.N., Mikhnevich S.Yu., Ermolaev I.E. *Opt. Spektrosk.*, **102** (1), 116 (2007).
24. Zemanek P., Jonas A. *J. Opt. Soc. Am. A*, **19** (5), 1025 (2002).
25. Palberg Th., Reiber H., Köller T., et al. arXiv:0811.2321v1.
26. Burkhanov I.S., Chaikov L.L., Korobov D.Yu., Krivokhizha S.V., Kudryavtseva A.D., Savranskiy V.V., Shevchuk A.S., Tcherniega N.V. *J. Russ. Laser Res.*, **33**, 496 (2012).
27. Burkhanov I.S., Chaikov L.L. *Proc. SPIE Int. Soc. Opt. Eng.*, **9066**, 906610 (2013).
28. Krivokhizha S.V., Lapteva E.S., Chaikov L.L., Shapovalova D.M. *Kr. Soobshch. Fiz. FIAN*, (11), 3 (2010) [*Bull. Lebedev Phys. Inst.*, **38** (4), 111 (2011)].
29. Odulov S.G., Soskin M.S., Khizhnyak A.I. *Lazery na dinamicheskikh reshetkakh* (Dynamic-Grating Lasers) (Moscow: Nauka, Fizmatlit, 1990).